# Recent Advances at the Globus-M2 Tokamak

ID: 3389


N.N. BAKHAREV, A.S. ALEXANDROV, S.E. ALEXANDROV, I.M. BALACHENKOV, M.K. BUTS, F.V. CHERNYSHEV, V.V. DYACHENKO, N.V. ERMAKOV, S.V. FILIPPOV, A.N. GOLYAKOV, V.YU. GORYAINOV, E.Z. GUSAKOV, V.K. GUSEV, A.YU. IVANOV, E.M. KHILKEVITCH, N.A. KHROMOV, E.O. KISELEV, A.N. KOVAL, A.N. KONOVALOV, S.V. KRIKUNOV, A.K. KRYZHANOVSKY, G.S. KURSKIEV, A.S. MAREEV, O.S. MEDVEDEV, A.D. MELNIK, V.B. MINAEV, I.V. MIROSHNIKOV, E.E. MUKHIN, A.N. NOVOKHATSKY, M.I. PATROV, YU.V. PETROV, A.YU. POPOV, A.G. RAZDOBARIN, N.V. SAKHAROV, A.E. SHEVELEV, P.B. SHCHEGOLEV, K.D. SHULYATIEV, O.M. SKREKEL, V.V. SOLOKHA, A.YU. TELNOVA, N.V. TEPLOVA, E.E. TKACHENKO, V.A. TOKAREV, S.YU. TOLSTYAKOV, G.A. TROSHIN, E.A. TYUKHMENEVA, V.I. VARFOLOMEEV, N.S. ZHILTSOV
Ioffe Institute, St.-Petersburg, Russia

E.G. KAVEEVA, K.A. KUKUSHKIN, A.M. PONOMARENKO, V.A. ROZHANSKY, I.YU. SENICHENKOV, A.Y. TOKAREV, A.Y. YASHIN
Peter the Great St. Petersburg Polytechnic University, St.-Petersburg, Russia

A.V. BONDAR, E.N. BONDARCHUK, A.A. KAVIN, I.V. KEDROV, A.B. MINEEV, V.N. TANCHUK, V.A. TROFIMOV, A.A. VORONOVA
JSC «NIIEFA», St.-Petersburg, Russia

P.A. BAGRYANSKY, S.V. IVANENKO, A.D. KHILCHENKO, A.N. KVASHNIN, E.I. PINZHENIN, I.V. SHIKHOVTSEV, A.L. SOLOMAKHIN
Budker Institute of Nuclear Physics, Novosibirsk, Russia

bakharev@mail.ioffe.ru

A.S. DZHURIK, YU.A. KASHCHUK, S.YU. OBUDOVSKY
Project Center ITER, Moscow, Russia

E.G. ZHILIN
Ioffe Fusion Technology Ltd., St.-Petersburg, Russia

A.E. KONKOV, P.S. KORENEV
V.A. Trapeznikov Institute of Control Sciences of Russian Academy of Sciences, Moscow, Russia

V.A. SOLOVEY
B.P. Konstantinov Petersburg Nuclear Physics Institute, Kurchatov Institute, St. Petersburg, Russia


## GLOBUS-M2

| Parameter | Value design/achieved |
|---|---|
| R [cm]/a [cm] | 36/24 = 1.5 |
| k | 2.0/2.1 |
| δ | 0.5/0.4 |
| $B_T$ [T] | 1/0.95 |
| $I_p$ [kA] | 500/450 |
| $t_{pulse}$ [ms] | 400/170 |
| $E_{NBI}$ [keV] | 30-50 |
| $P_{NBI}$ [MW] | 2/2 |
| ICRH [MW] | 0.5/0.1 |
| LHCD [MW] | 0.5/0.2 |
| Max $T_i$, [keV] | 4.7 at $\langle n_e\rangle_l=5\cdot10^{19}m^{-3}$ |
| Max $T_e$ [keV] | 1.8 at $\langle n_e\rangle_l=5\cdot10^{19}m^{-3}$ |

**Extreme specific heating power ≈4 MW/m³**

## BORONIZATION

**New boronization technique (ISB) was utilized during the 2024-2025 campaign.**
Significant advantage over conventional glow discharge boronization (GDB).
Technique:

- vessel with carborane ($B_{10}H_{12}C_2$) connected to tokamak – gas inflow between shots.
- Boronization is happening in the initial phase of the discharge->doesn't affect plateau

$Z_{eff}$ decreases during ISB

$U_p$ and impurity lines demonstrate similar behaviour.

$Z_{eff}$ < 1.1 during NBI in C-wall tokamak

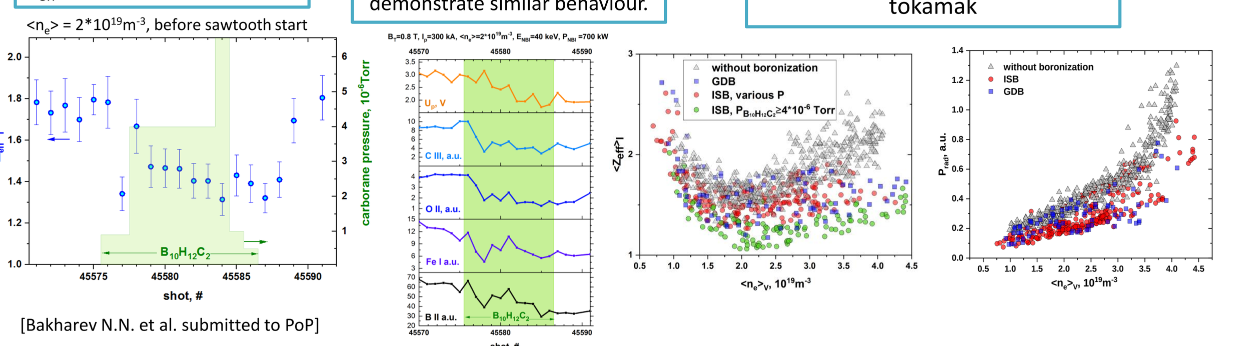

[Bakharev N.N. et al. submitted to PoP]

DD Neutron rate doubling

Fast ion confinement improvement

Same stored energy at lower $P_{OH}$
But at higher $P_{NBI}$

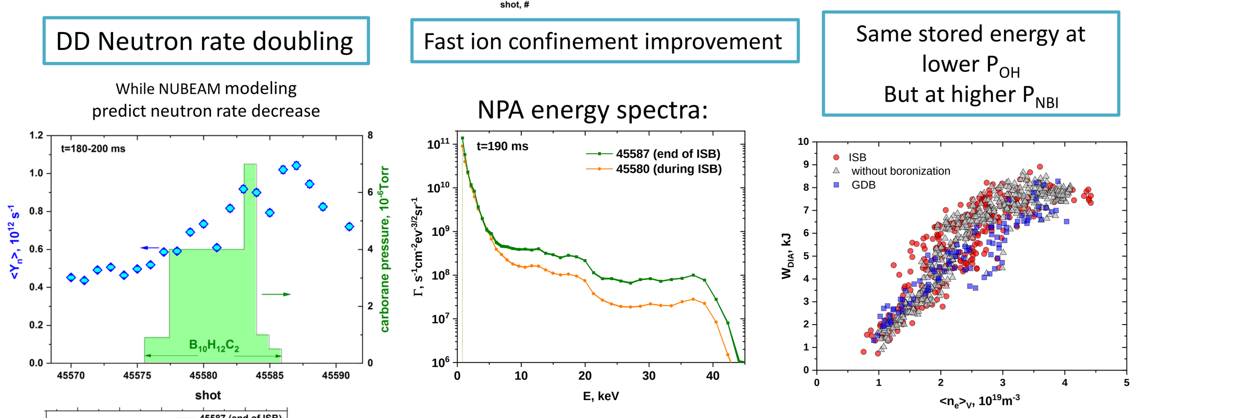

No energy confinement change
As compared to the case without boronization $\tau_E$~12 ms ($\langle n_e\rangle_V$≈3·10¹⁹m⁻³) is consistent with Glb-21 scaling

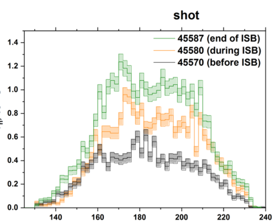

For the same $n_e$ #41570 vs #41580:

- NUBEAM simulation: 30% $Y_n$ decrease
- Experiment: 60% $Y_n$ increase

Most probable explanation: decrease of Charge-Exchange losses

## SOL

High Field Side High Density feature has been discovered in Globus-M2 using divertor TS [Mukhin E.E. , EX-D, P2]

$n_e$ at the inner divertor leg 1.5-3x higher than in midplane

Observed over a wide range of discharge parameters: $n_e(0)$: 2·10¹⁹-1.4·10²⁰ m⁻³ with and without NBI

SOLPS-ITER simulation taking into account drifts experiment

ExB drift in the HFS direction leads to the formation of a HFSHD

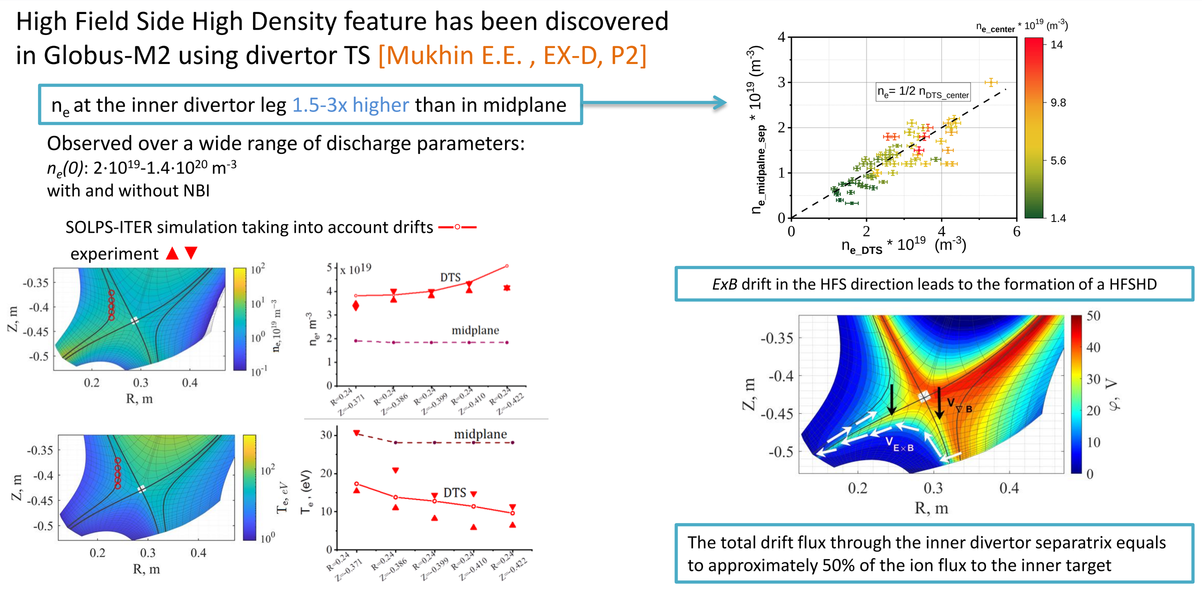

The total drift flux through the inner divertor separatrix equals to approximately 50% of the ion flux to the inner target

SOL power decay length $\lambda_q$ was measured using IR thermography
$B_T$=0.5-0.95 T, $I_p$=155-400 kA, up to 0.8 MW NBI

Comparison with multi-machine scaling [Eich T. et al 2013 Nucl. Fusion **53** 093031]

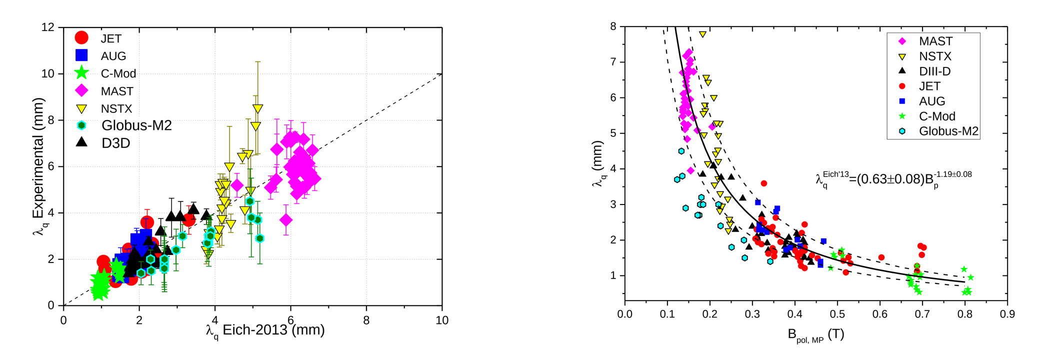

$\lambda_q^{Globus-M2} \sim B_p^{-1}$ in ST with $B_T$ up to 0.95 T and $\lambda_q$~2mm, confirming data from conventional devices ($\lambda_q \sim B_p^{-1.19}$)

## Globus-3

**Globus-3 is the next step ST in Ioffe institute.**
[Minaev V.B. PWF-P2]

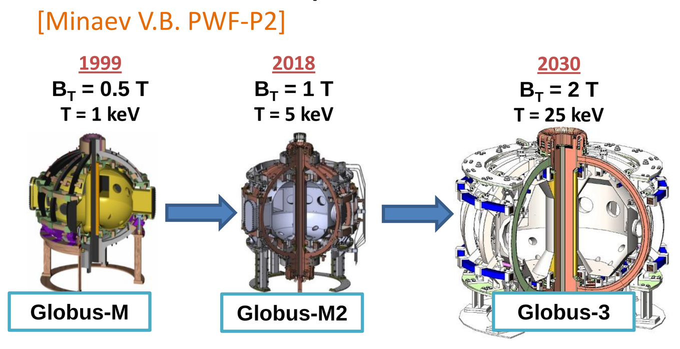


- **Design implements Globus-M and Globus-M2 solutions, while correcting their design flaws**
- **The project is aiming to achieve thermonuclear plasma (simultaneous $T_{i0}$~25 keV, $\langle n_e\rangle$~10²⁰m⁻³)**
- **Globus-3 will be a tokamak with the highest $P_{aux}$/V = 3-4 MW/m³ in the world.**

| Parameter | Globus-M | Globus-M2 | Globus-3 |
|---|---|---|---|
| R, m/a, m | 0.36/0.24=1.5 | | **0.775/0.44=1.76** |
| $B_T$, T | 0.4 | 1 | **2** |
| $I_p$, MA | 0.2 | 0.5 | **2** |
| t pulse, s | 0.1 | 0.4 | **3** |
| NBI, MW | 1 | 2 | **11.5 (14)** |

**Timeline:**

- Conceptual design – 2025 – 2026
- Detailed design – 2026 – 2027
- Manufacturing of EMS and VV – 2027-2029
- Modernization of the power supply system – 2029 – 2031
- Assembling the Globus-3 – 2030
- Start-up of the tokamak with the existing heating and diagnostics systems - 2031

Transport modeling with ASTRA

**$\langle n_e\rangle_V$=10²⁰m⁻³, 11.5 MW 60 keV NBI,** Hot-ion mode, neoclassical ion transport

**Base scenario, H-factor=1** **Upside scenario, H-factor=2**

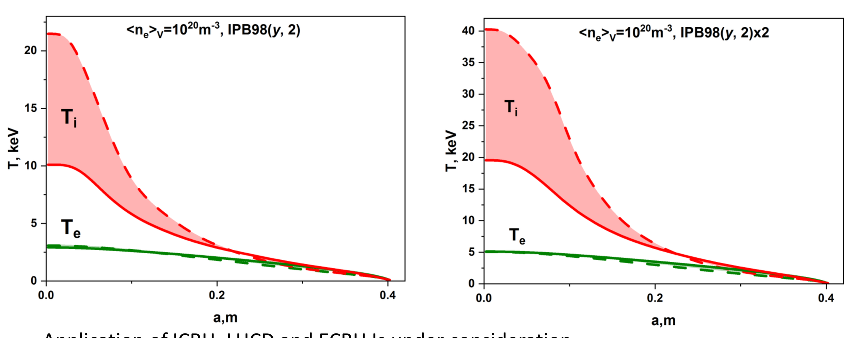

α-particle studies ¹¹B(p, α)2α : 10¹¹ s⁻¹-10¹⁴ s⁻¹ accceptable for experimental studies

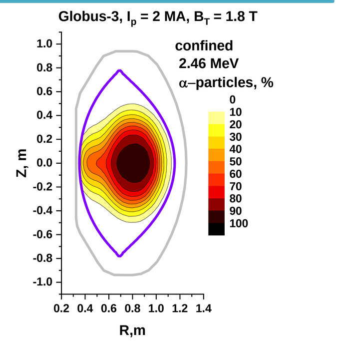

Application of ICRH, LHCD and ECRH is under consideration.

## NEW DIAGNOSTICS AND CONTROL

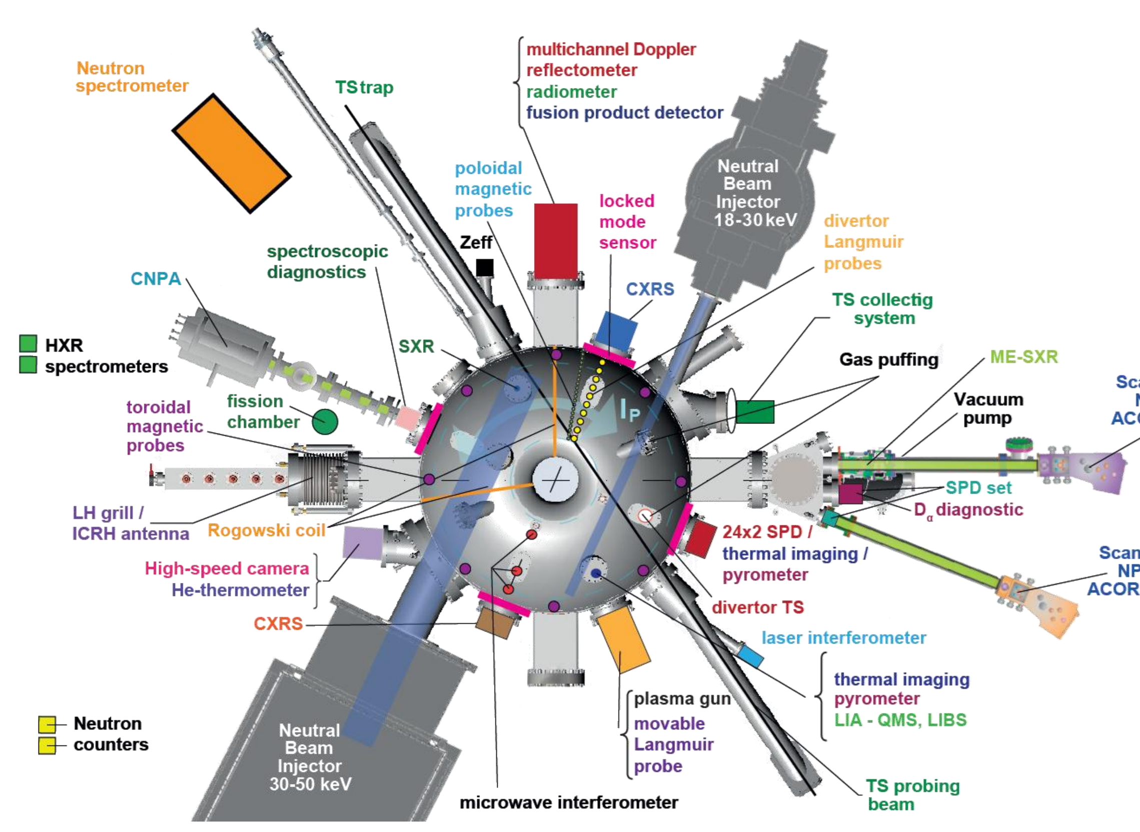

- **dispersion interferometer**
[IVANENKO, S.V. et. al., Fus.Eng.Des. 202 (2024) 114409]
- **charged fusion product detector from Budker institute**
[BAKHAREV, N. N., et al. Tech. Phys. Lett. **50** 10 (2024) 24-27.]
- **two-color pyrometer**
[VORONIN, A. V., et al. Tech. Phys. 68 12 (2023) 799-805 ],
- **locked-mode sensor**
[PETROV, Y. V., et al., Plasma Phys. Rep.. **50** 7 (2024) 773-780.]
- **high-speed cameras** [TIMOKHIN, V., EX-E P4]
- **Silicon Precision Detector array**
- **Real time Plasma EQ and control**
(under implementation)
[KORENEV, P. S., et al. Tech, Phys, Lett. **49** 4 (2023) 372-375.]
- **LIA-QMS, LIBS**
[RAZDOBARIN, A.G. et al. Plasma Phys. Rep. **50** 6 (2024) 667–677][O.S. MEDVEDEV, et al., Nucl. Mater. and Energy. **41** (2024) 101829.]
- **$U^{235}$&$U^{238}$ neutron cameras**
[KORMILITSYN TEC-FNT, P6]
- **Divertor Thomson Scattering**
[ERMAKOV, N. V., et al., Plasma Phys. Rep. 49 12 (2023) 1480]

ITER Tech.

[ERMAKOV, N. V., et al., Plasma Phys. Rep. 49 12 (2023) 1480]
[MUKHIN E.E. EX-D, P2]

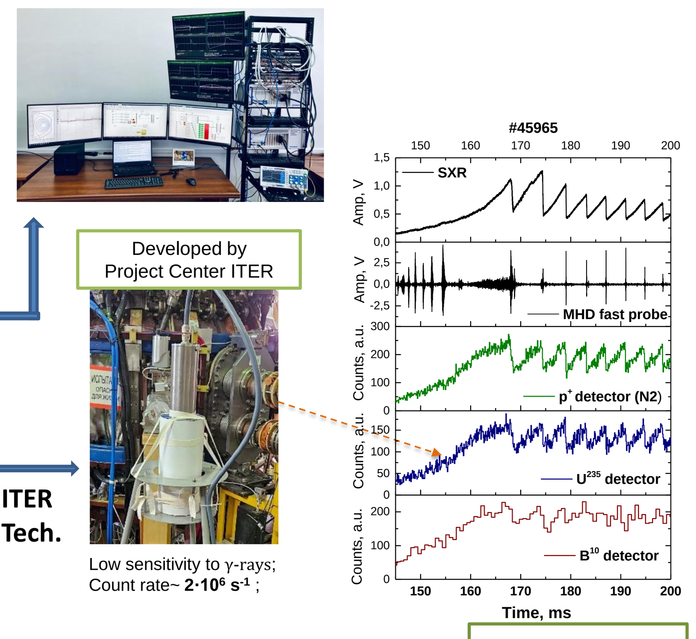

Developed by Project Center ITER

Low sensitivity to γ-rays; Count rate~ 2·10⁶ s⁻¹

Applicability of the TS hardware in the tokamak control system was demonstrated: $\Delta\tau$ < 1 ms.

[ZHILTSOV, N. S. et al. Tech. Phys. Lett., **49** 8 (2023) 350-354.]

Precise (~0.1mm) online alignment of the TS diagnostics was implemented in the equatorial TS.

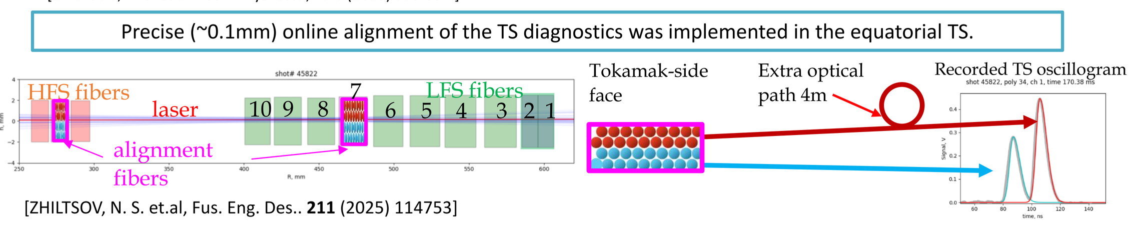

[ZHILTSOV, N. S. et.al, Fus. Eng. Des.. **211** (2025) 114753]

Laser-Induced Ablation + Quadrupole Mass-Spectrometry – **in-situ** layer-by layer H/D concentration
Laser-Induced Breakdown Spectroscopy-Elemental composition with ~500 nm depth resolution
[RAZDOBARIN, A.G. et al. Plasma Phys. Rep. **50** 6 (2024) 667–677] [O.S. MEDVEDEV, et al., Nucl. Mater. and Energy. **41** (2024) 101829.]

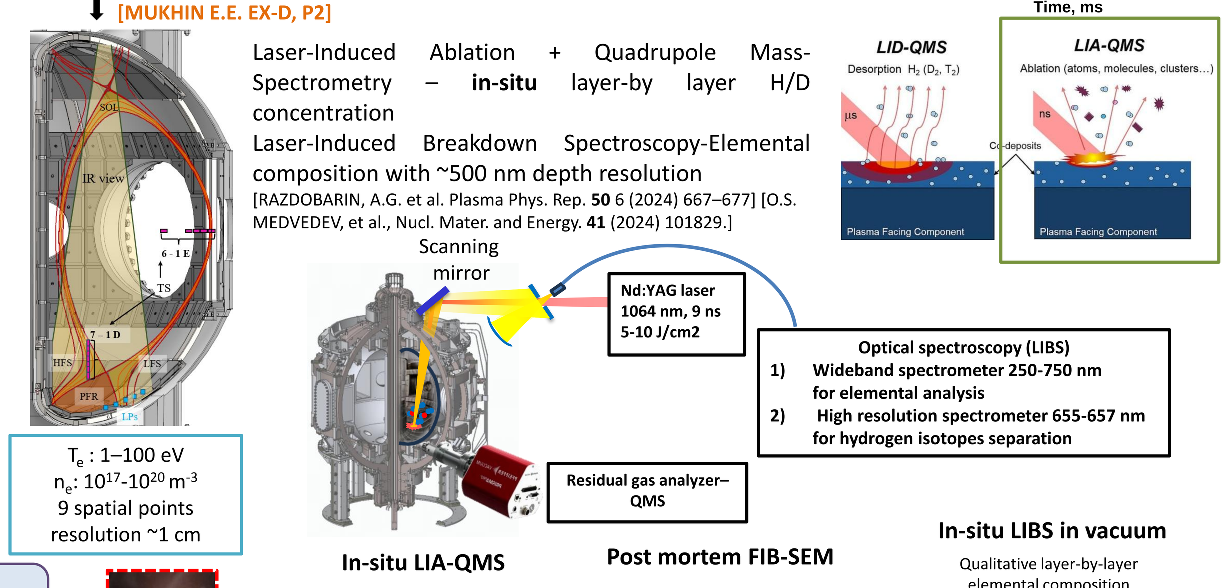

$T_e$ : 1–100 eV
$n_e$: 10¹⁷-10²⁰ m⁻³
9 spatial points
resolution ~1 cm

In-situ LIA-QMS   Post mortem FIB-SEM   In-situ LIBS in vacuum

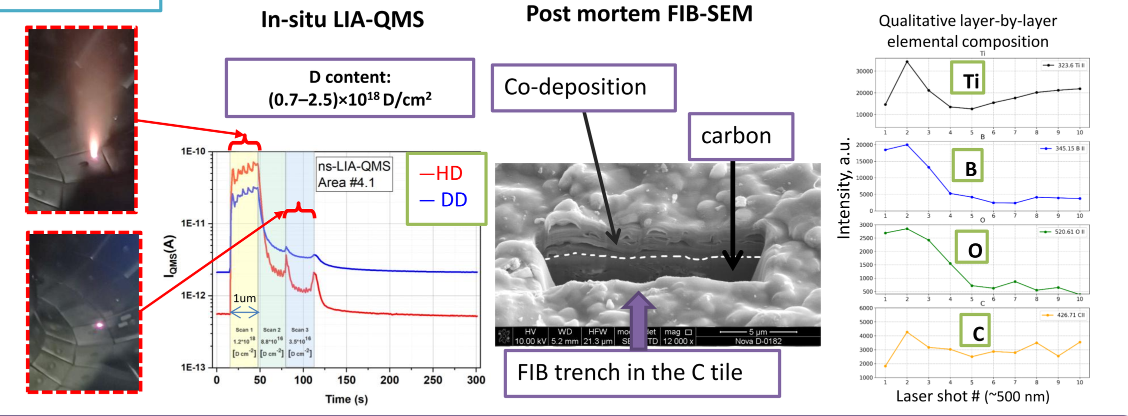

## HOT ION MODE

Hot-ion mode - a natural operating regime of Globus-M2 during H and D NBI in D plasma at $B_T$≥ 0.7 T. [Kurskiev, G.S., EX-H P4] [G. S. Kurskiev et al. Plasma Phys. Rep. 49, 403–418 (2023)] [Kiselev, E.O., EX-C P1]

MAX $T_i$(0)
D NBI: 4.7 keV
H NBI: 2.9 keV

$B_T$=0.8-0.9T
$I_p$=300-400 kA

D NBI   ASTRA modeling   H NBI

Neoclassical ion transport   Anomalous ion transport

$\tau_E$ = 14 ms   $\tau_E$ = 7 ms

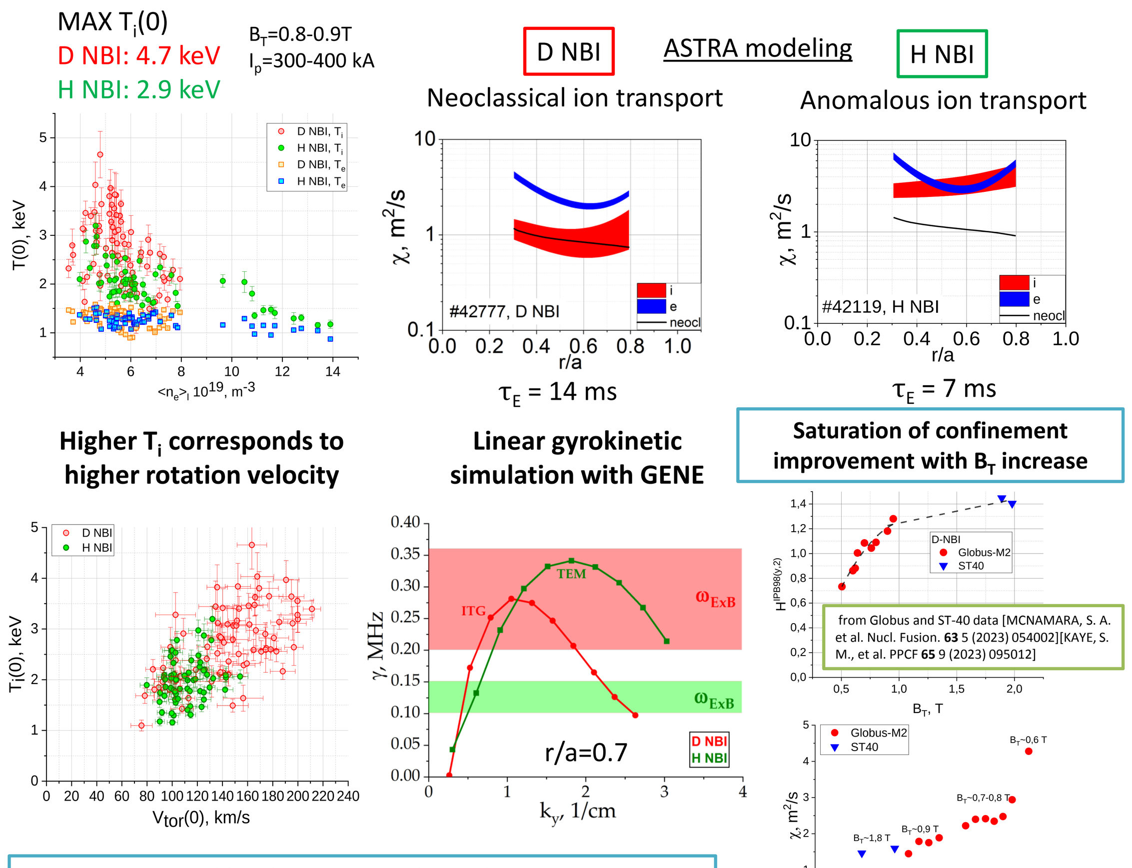

Higher $T_i$ corresponds to higher rotation velocity

Linear gyrokinetic simulation with GENE

Saturation of confinement improvement with $B_T$ increase

ITG is suppressed by the rotation shear during D NBI
During H NBI rotation is not enough to suppress TEM

## ICRH

During Globus-M2 2024 campaign the novel experiments with ICRH in Minority Heating and 2nd harmonic regimes at $B_T$=0.7 T. Absorbed power ~50 kW.
MH experiments showed 15% increase in T at $X_H$~20%.
2nd harm. NBI+ICRH showed 10x growth of $n_D$ with E> $E_{NBI}$

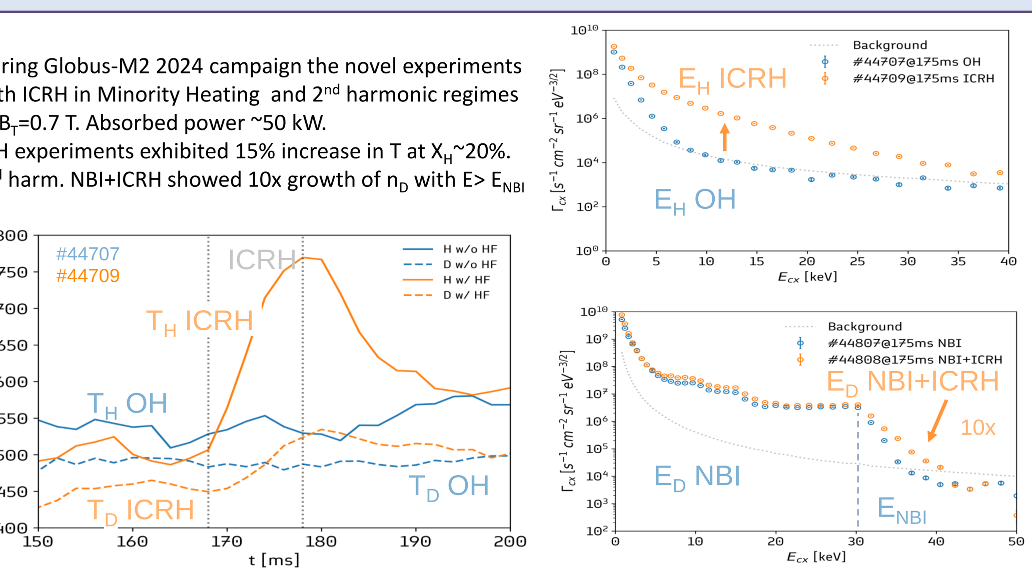

## ELMs

During small ELMs significant $T_e$ changes inside the separatrix are not observed

Fast particle losses associated with ELMs are found

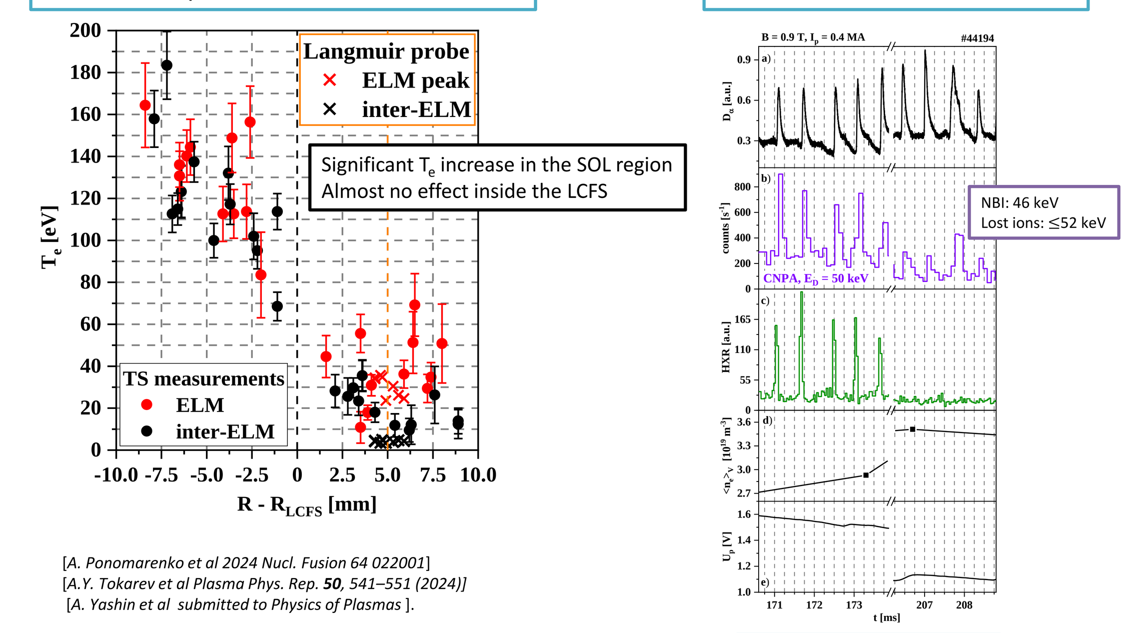

[A. Ponomarenko et al 2024 Nucl. Fusion 64 022001]
[A.Y. Yokarev et al Plasma Phys. Rep. 50, 541–551 (2024)]
[A. Yashin et al submitted to Physics of Plasmas ].

Triangularity was varied from 0.4 to 0.2
[Solokha V.V. TH-S, P7]

ELM-free regime with EHO was observed
[Yashin A. Yu. EX-E, P4]

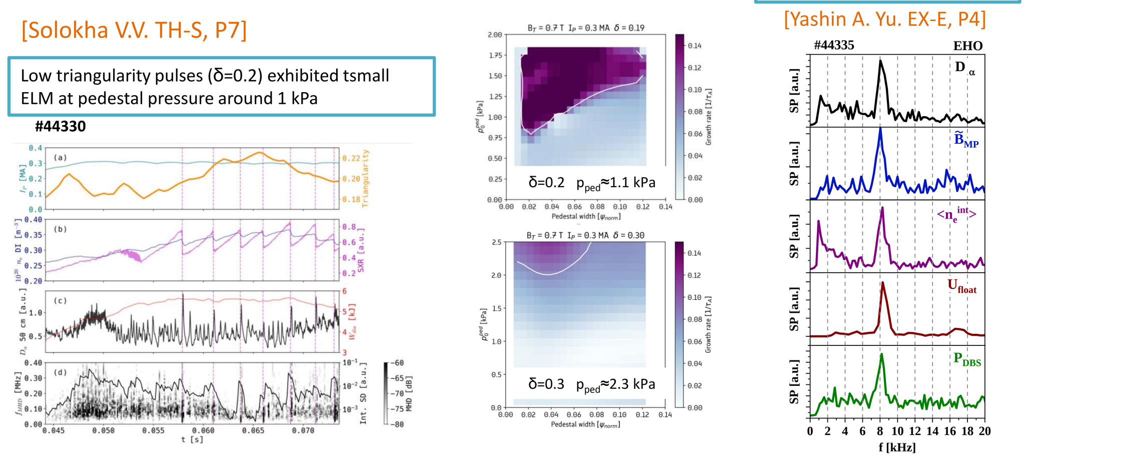

The 3-field linear MHD simulations using BOUT++ showed low-δ PB to have peeling traits and mode structure located near separatrix, while mid-δ PB have more ballooning properties and wider structure.

## ALFVÉN INSTABILITIES

Alfvén-type instabilities exists in a wide range of experimental parameters

Improved plasma parameters and fast-ion confinement ⇒ previously unobserved **EPM**s

Multi-frequency Doppler backscattering method demonstrated localization close to the magnetic axis (R~0.42 m)

[PONOMARENKO A. EX-W, P4]

EPM-induced fast ion transport and losses were observed for the first time Up to 30 MW **MW/m²** wall load

Up to **20 MW/m²** local fast ion wall load during **TAE** was observed

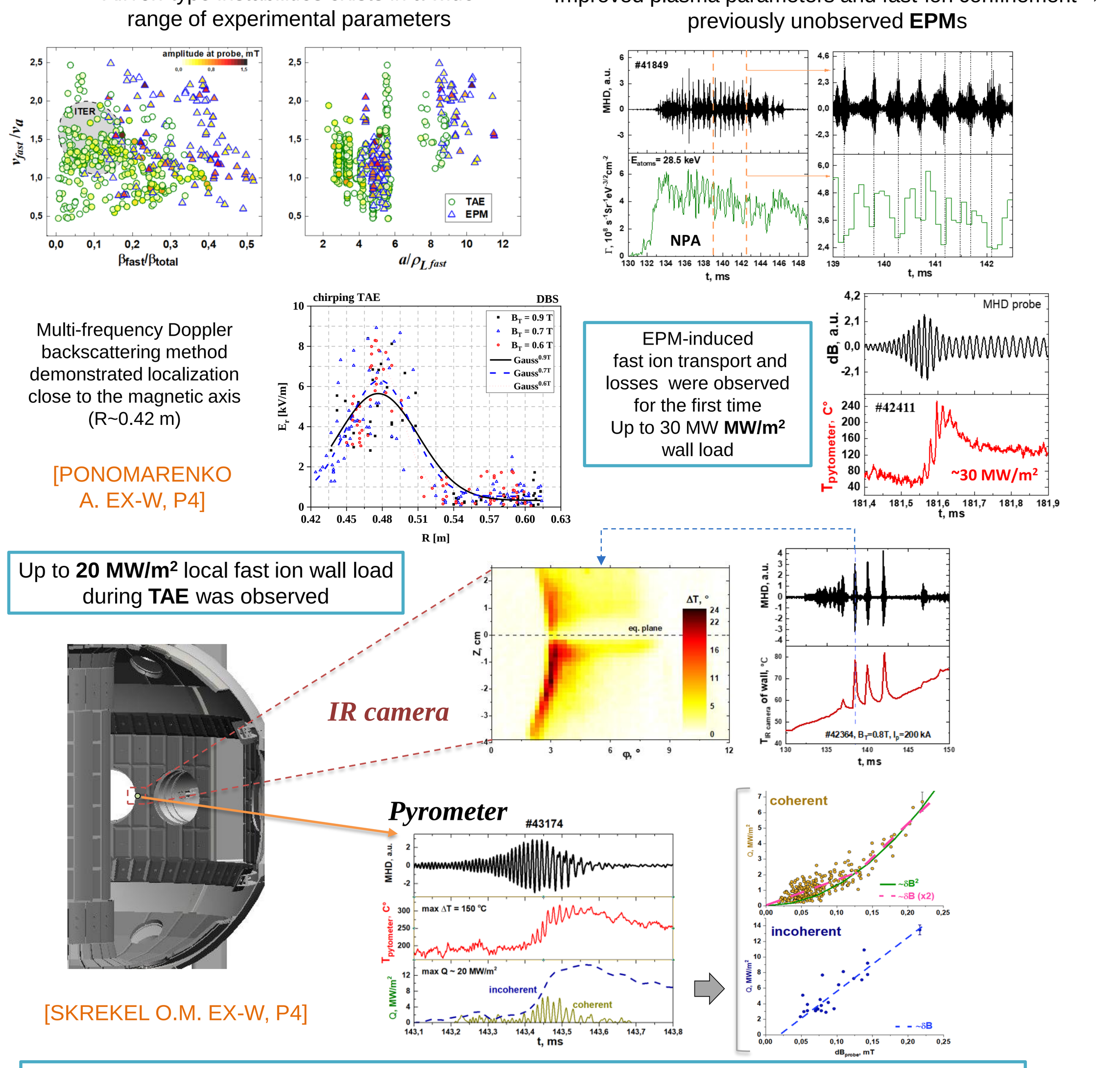

[SKREKEL O.M. EX-W, P4]

Both coherent and incoherent components are associated with the convective transport but different type of losses: orbital and CX respectively.

## OBSERVATION OF HIGH FREQUENCY INSTABILITIES

Ion-cyclotron emission was observed during NBI
[M. S. Kulygin,et., al., Tech. Physics Letters 50(9) 71 (2024)]

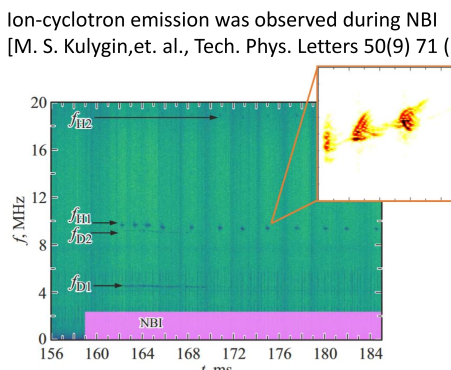

The resonance was found to be located in the plasma bulk close to magnetic axis which indicates that the instability drive is rather due to interacion with shear Alfven wave (ion cyclotron wave) than fast magnetosonic.

Fast Magnetosonic waves driven by energetic electrons in OH discharges
[I. M. Balachenkov, Plasma Sci. Technol 25 075102 (2023)]

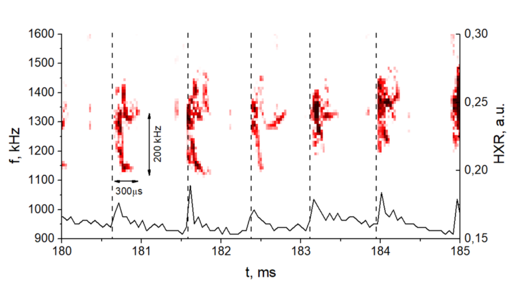

Longitudinally polarized chirped oscillation bursts, having their frequency following the Alfvén scaling, correlated with the moments of MHD n = 1 sawtooth disruptions.

High-Frequency electron-beam driven magnetosonic whistler was observed.
Instability exists at low plasma densities $\langle n_e\rangle$ < 2 × 10¹⁸ m⁻³ or even after the end of plasma current

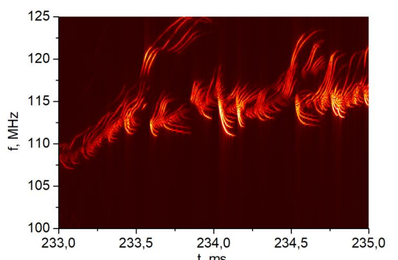

## ACKNOWLEDGEMENTS


The work was performed on the Unique Scientific Facility "Spherical tokamak Globus-M". Preparation of the routine tokamak diagnostics (section 2) was performed in accordance with the state assignment № FFUG-2021-0001. Wall conditioning studies (section 3) was performed in accordance with the state assignment № FFUG-2024-0028. Fast ion study (subsection 6.1, 6.6) was supported by RSF research project № 24-12-00162. Work on the study of divertor plasma (subsection 5.2) was supported by the Russian Science Foundation (23-79-00033). ELM and EHO studies (subsection 6.2, 6.3) were supported by RSF research project № 21-79-20133-P. Energy confinement studies (subsection 4.1) were supported by RSF research project № 21-72-20007-P. Globus-3 development was supported by RSF research project № 21-79-20133-P.